LOCALIZED EXCITONS IN InGaN

S. CHICHIBU*, T. DEGUCHI**, T. SOTA**, K. WADA***, S. NAKAMURA****
*Materials Department, University of California, Santa Barbara, CA 93106, and also Faculty of Science and Technology, Science University of Tokyo, 2641 Yamazaki, Noda, Chiba 278, Japan
**Department of Electrical, Electronics, and Computer Engineering, Waseda University, 3-4-1 Ohkubo, Shinjuku, Tokyo 169, Japan
***Compound Semiconductor Materials Research, NTT System Electronics Laboratories, 3-1 Morinosato-Wakamiya, Atsugi, Kanagawa 243-01, Japan
****Department of Research and Development, Nichia Chemical Industries Ltd., 491 Oka, Kaminaka, Anan, Tokushima 774, Japan

ABSTRACT

Emission mechanisms of the device-quality quantum well (QW) structure and bulk three dimensional (3D) InGaN materials grown on sapphire substrates without any epitaxial lateral overgrown GaN (ELOG) base layers were investigated. The $In_xGa_{1-x}N$ layers showed various degree of spatial potential (bandgap) fluctuation, which is probably due to a compositional inhomogeneity or monolayer thickness fluctuation produced by some kinetic driving forces initiated by the threading dislocations (TDs) or growth steps during the growth. The degree of fluctuation changed remarkably around nominal InN molar fraction x=0.2, which changes to nearly 8-10 % for the strained $In_xGa_{1-x}N$. This potential fluctuation induces energy tail states both in QW and 3D InGaN, showing a large Stokes-like shift combined with the red shift due to quantum confined Stark effect (QCSE) induced by the piezoelectric field. The spontaneous emission from undoped InGaN single quantum well (SQW) light-emitting diodes (LED's), undoped 3D double heterostructure (DH) LED's, and multiple quantum well (MQW) laser diode (LD) wafers was assigned as being due to the recombination of excitons localized at the potential minima, whose area was determined by cathodoluminescence (CL) mapping to vary from less than 60 nm to 300 nm in lateral size in the case of QW's. The lasing mechanisms of the cw $In_{0.15}Ga_{0.85}N$ MQW LD's having small potential fluctuation, whose bandgap broadenings are less than about 50 meV, can be described by the well-known electron-hole-plasma (EHP) picture with Coulomb enhancement. The inhomogenous MQW LD's are considered to lase by EHP in segmented QW's or Q-disks. It is desirable to use entire QW planes with small potential inhomogeneity as gain media for higher performance LD operation.

INTRODUCTION

The InGaN alloys are attracting special interest because of their potential for the fabrication of light emitting devices operating in the red to ultraviolet (UV) energy region. Bright blue, bluish-green, and pure green LED's have been put into practical use [1], and the device lifetime of a cw operation of purplish-blue MQW LD's with modulation-doped strained-layer superlattice (MD-SLS) cladding layers grown on ELOG substrates extended up to 10,000 hours at room temperature (RT), as estimated from accelerated testing [1]. All the good performance blue/green LED's [1] and purplish-blue or UV LD's [1-6] reported to date have InGaN active layers. However, the material physics in InGaN is still unclear. One of the important issues in InGaN material is its phase-separating nature [7-9] due to mismatch of thermodynamical and chemical stabilities between GaN and InN. A strong piezoelectric field in strained InGaN also affects the optical properties [10]. The practical LED's and LD's grown on sapphire substrates have large TD densities up to 10^9 cm^{-2} [1]. However, they exhibit intense electroluminescence (EL) peaks or lasing operation. Thus we have started our research work in order to clarify the emission mechanisms of InGaN-based QW and DH structures for further improvement of the device performances. Since 3D wurzite GaN exhibits an excitonic photoluminescence (PL) peak even at RT [11,12], it has been also important to investigate the contribution of excitons on the spontaneous EL peak from InGaN QW structures and 3D epilayers.

This report presents experimental results on optical and structural properties of device quality InGaN SQW, MQW, and 3D layers grown on sapphire (0001) substrates with a low-temperature GaN buffer layer [1] only. The spontaneous emissions from them are assigned as being due to the recombination of excitons spatially localized at potential minima [13,14] whose lateral sizes varied from less than 60 nm to up to 300 nm [14] due to the potential inhomogeneity [13-17]. Their sizes correspond to structures that are referred to as quantum-disks (Q-disks) [18] and segmented quantum wells (SgQW's) depending on the lateral size. The

Mat. Res. Soc. Symp. Proc. Vol. 482 © 1998 Materials Research Society

lasing mechanisms of cw $In_{0.15}Ga_{0.85}N$ MQW LD's having small potential undulations are well explained by the EHP picture with strong Coulomb enhancement [19]. However, those LD's having inhomogeneous MQW's exhibited characteristic gain peaks.

EXPERIMENT

Samples used in this study were grown on sapphire (0001) substrates by metalorganic vapor phase epitaxy (MOVPE) with low-temperature GaN buffer layers [1].

The AlGaN/InGaN 3D DH LED structures [1] were modified to have (i) a 50 nm-thick $In_{0.06}Ga_{0.94}N$ active layer codoped with Si and Zn, (ii) the same structure as (i) except for an undoped $In_{0.06}Ga_{0.94}N$ active layer, (iii) the same structure as (i) except for a Si-doped (10^{19} cm^{-3}) $In_{0.06}Ga_{0.94}N$ active layer. For PL and PL excitation (PLE) measurements, a 50 nm-thick undoped 3D $In_{0.09}Ga_{0.91}N$ layer was grown on a 50-nm-thick $In_{0.01}Ga_{0.99}N$:Si / 50-nm-thick $Al_{0.3}Ga_{0.7}N$:Si / 2-μm-thick GaN:Si epilayer base.

The blue/green SQW LED's have a 3 nm-thick undoped $In_xGa_{1-x}N$ QW (x=0.3 and 0.45), respectively [1]. For both spatially-resolved and integrated CL measurements, 3 nm-thick undoped $In_xGa_{1-x}N$ (x=0.05, 0.2, and 0.5) SQW's were grown on a 3-μm-thick Si-doped (5×10^{18} cm^{-3}) GaN layer. The SQW's were subsequently capped by a 6 nm-thick undoped GaN layer, or uncapped.

Several MQW LD wafers [1] were prepared. One of them has ten periods of 2.5 nm-thick $In_{0.2}Ga_{0.8}N$ wells and 7.5 nm-thick $In_{0.05}Ga_{0.95}N$ barriers, whose pulsed lasing wavelength is 410 nm and the spontaneous EL peak is 399 nm (3.11 eV) at RT [1,13]. Its threshold current density (J_{th}) was 11.4 kA/cm^2. The other cw LD wafer group had three 3.5 nm-thick $In_{0.15}Ga_{0.85}N$ wells. Two LD wafers were examined, namely CW1 and CW2. A remarkable difference between the two is that the potential fluctuation in the QW plane in CW1 is much weaker than that in CW2. The J_{th} for RT cw operation were 7.4 and 9.4 kA/cm^2, and the wavelength was 398 and 409 nm for CW1 and CW2, respectively. The device lifetime was less than 1 hour for both LD's. As shown later, CW1 has small potential fluctuation, and showed a gain spectrum that can be fully explained by the EHP picture.

EL and photovoltage (PV) spectra were measured using the LED or LD devices. PL, PLE, and modulated-electroabsorption (EA) spectra [13] were measured using the device wafers. For comparison, we also characterized single GaN epilayers by the photoreflectance (PR) measurements [20]. Both the PR and EA spectra were analyzed using the Lorentzian lineshape functional form. Static PL was mainly excited by the 325 nm line of a cw He-Cd laser. Time-resolved PL (TR-PL) measurements were also carried out using a N_2 pulsed laser or a frequency-doubled Ti:sapphire laser as an exciter. These measurements were carried out between 10 K and RT.

Spatially-integrated or spatially-resolved CL [15] was excited by a cw electron beam (e-beam) with or without the e-beam scanning, and dispersed by a 25 cm focal-length grating monochromator coupled to a scanning electron microscope. The energy resolution of the CL spectrum was about 15 meV at 410 nm. The acceleration energy and current of e-beam were typically 3 kV and 20 pA, respectively. Monochromatic spatially-resolved CL images were taken under a fixed wavelength with the e-beam scanning. The spatial resolution of the CL mapping is essentially limited by the diffusion length in the matrix, which corresponds approximately to less than 60 nm in this experiment, judged from the minimum dark area width. All CL measurements were carried out at 10 K.

To study gain spectra, spectral-resolved emission signals were measured using the variable excitation-stripe length optical pumping (VEL) method [21]. The excitation light was obtained from a frequency-tripled 10 Hz Q-switched Nd^+:YAG laser with a pulse duration of 10 ns. The excitation wavelength 355 nm nearly matches the exciton resonance energy of GaN at RT. The net modal gain, g(E), is obtained by measuring the stimulated intensity as functions of stripe length and pumping power intensity [22].

RESULTS AND DISCUSSION

Excitonic Structures in GaN

In this section RT excitonic features in optical spectra of GaN are described as background to this work. The optical absorption (OA), PR, and PL spectra of a GaN epilayer measured at RT are summarized in Fig. 1 [11]. A clear excitonic resonance is found in both OA and PR spectra. Indeed, the resonance structures consist of two free excitonic (FE) resonances related to A and B transitions [FE(A) and FE(B), respectively]. The PL peak is a convolution of FE(A) and FE(B) emissions [11]. It is natural to observe FE emission from 3D GaN at RT, since this material satisfies several restrictions for excitons to survive at RT; (1) small numbers of active LO phonons at RT, which is satisfied if the LO phonon energy is far larger than the thermal energy k_BT of RT (26 meV), and (2) large binding energy of FE's greater than k_BT. Other two restrictions depend on the injected carrier density and the device structure; (3) exciton Bohr radius a_B smaller than the screening length, which is satisfied if the charge density is smaller than the critical charge density N_{crit} [19] and (4) the electric field is weaker than the critical value (E_{ex}/a_B). The former two are easily satisfied, because the LO phonon energies in GaN are very large [91 meV for A_1(LO) mode and 93 meV for E_1(LO) mode] [23] and few LO phonons are thermally activated even at RT [24]. Also, GaN has a large E_{ex} of 26 meV [25], which is comparable to k_BT. The small dielectric constant (ε=8.2) [25] and a_B (3.4 nm) [25], and large effective masses [26] lead to N_{crit} as high as 1×10^{18} cm^{-3} according to Debye-Huckel screening [19]. Furthermore, the critical electric field strength is calculated to be 7.6×10^4 V/cm, which means that excitons in GaN are field-resistant particles. These *excitonic* material properties, which come from the strong Coulomb interaction in GaN, make it possible to observe FE emissions at RT [11,12].

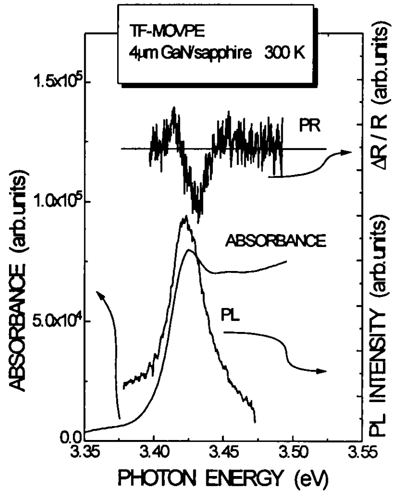

Fig. 1 Free exciton emission in 3D GaN (RT).

Optical properties of InGaN QW's

Figure 2 summarizes the spontaneous EL, PV, and EA spectra of SQW (x=0.3, 0.45) and MQW (x=0.2) LED's at RT. The EA spectra exhibit a derivative-like resonance structure. Because the broadening parameter Γ [20] of the structures are very large, the structures due to the A- and B-transitions [25-28] are not resolved. The EA measurement monitors the FE resonance rather than band-to-band transitions even at RT in wide gap semiconductors provided that a_B is small [11,13,20,25,29]. Therefore each PV peak and EA resonance corresponds to FE absorption in the QW. The result that the PV spectra exhibit a peak-like line shape also supports that the FE resonance is observable at RT. The PV peak energy decreases from 3.21 to 2.91 eV with increasing x from 0.2 to 0.3. However, the peak energy is nearly unchanged for x=0.3 and x=0.45, and the full width at half maximum (FWHM) of all structures seem to increase with increasing x. These broadened EA and PV structures are discussed later. The spontaneous EL peak is located at the lower energy tail of the FE resonance, exhibiting the large Stokes-like shift in QW's.

The relation between the Stokes-like shifts and x is shown in Figs. 3 and 4. As shown in Fig. 3, the energy difference between the FE resonance and the emission increases with increasing x both in the QW's and 3D layers. The longer component of the decay time obtained by the TR-PL measurements also increases with increasing x. Such increase of the decay time is one of the characteristics of localized electronic systems [18], and detailed TR-PL measurements have been done by Narukawa *et al.* [14] and Hangleiter *et al.* [30]. However, further experiments are necessary to explain the long decay time; e.g., enhancement of the decay time by the piezoelectric field should be taken into account.

It should be mentioned here that there is a certain critical InN molar fraction, nominally nearly x=0.2, where the dependences of the FE resonance, Stokes-like shift, and

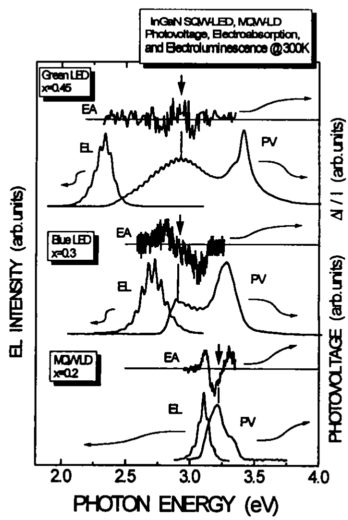

Fig. 2 Optical properties of InGaN QW's

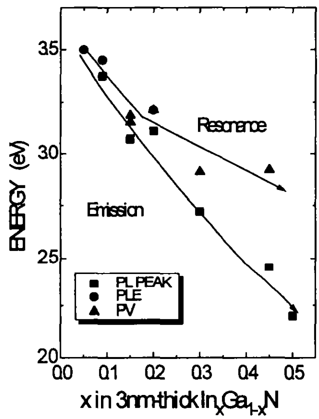

Fig. 3 Resonance and emision energies in InGaN QW's as a function of x.

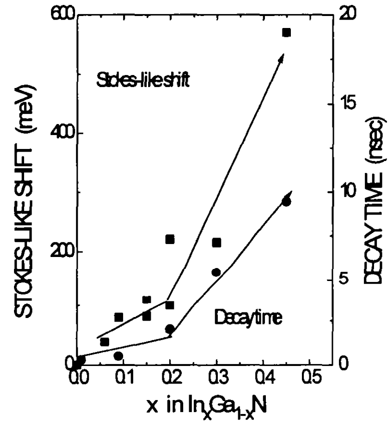

Fig. 4 Stokes-like shift and decay time of InGaN as a function of x.

decay time on x change remarkably. Especially, the Stokes-like shift increases rapidly for x>0.2. The 3 nm-thick well width MQW LD structure with x=0.2 exhibited a Stokes-like shift of 100 meV [13], however, other 3 nm-thick QW samples with x=0.2 exhibited a larger Stokes-like shift of 250 meV [14,15]. This means that the degree of the potential fluctuation changes around x=0.2, which can explain the inconsistency between the results of Narukawa *et al.* [14] and ours [13,15], which has been argued before. The $In_xGa_{1-x}N$ layers having x>0.2 are considered to have some extra mechanisms for producing the Stokes-like shifts.

Recently, Takeuchi *et al.* [10] reported that AlGaN and InGaN alloys grew coherently on thick GaN layers at least up to the thicknesses of 650 and 40 nm, repsectively. Therefore, x values in strained InGaN layer, especially QW's, must be carefully estimated. If this is also the case for our InGaN samples, the x values may be modified to about half of the original values determined by the x-ray diffraction (XRD) measurements, according to their reliable bowing parameter for strained InGaN (3.2 eV) [10]. Then the critical x is changed to be about 8-10 %, which agrees with the critical value calculated theoretically [7-9] from thermodynamics and kinetics.

Origin of the Stokes-like shift in InGaN QW's

Possible origins of the Stokes-like shift observed in QW's are shown schematically in Fig. 5. Usually, the energy difference between the absorption and emission is caused by the potential inhomogeneity in the active layer originating from several reasons listed in Fig. 5. In hexagonal nitirides, however, QCSE owing to the piezoelectric field in the (0001)-oriented strained QW's [31,10,13] should be considered as well as that due to the built-in field. It was reported that the directions of the piezoelectric and built-in field are opposite [10]. Thus both effects are estimated as follows. Since the QW's are very thin (3 nm) and both n-GaN and p-$Al_{0.2}Ga_{0.8}N$ barriers are highly-doped, a strong built-in electric field exists across the QW plane. The field strength is as high as 8.5×10^5 V/cm, which is estimated from the values of electron and hole concentrations in n- and p-type barriers (5×10^{18} cm^{-3} and 1×10^{18} cm^{-3}, respectively). The piezoelectric field strength in 1% strained GaN QW is estimated to be of the order of MV/cm [10.32], and the Stark shift due to QCSE in 3 nm-thick QW is estimated to be 26 meV and 274 meV for the field's of 1 MV/cm and 4 MV/cm [13,32], respectively.

Figure 6 shows PL spectra at RT of an $In_{0.45}Ga_{0.55}N$ SQW LED structure as a function of external bias. The PL was excited by the 457.9 nm (2.71 eV) line of a cw Ar^+ laser (50 mW), which excites carriers only in the SQW. The peak intensity decreases with increasing reverse bias. The PL spectrum for V=+1.991 V

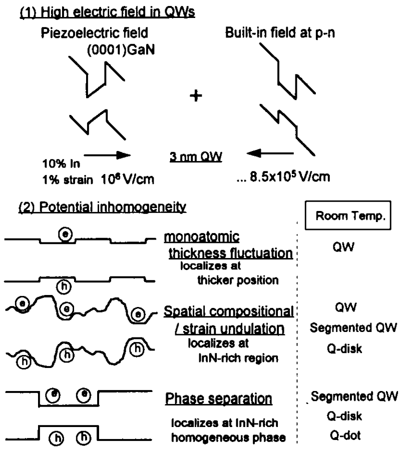

Fig. 5 Schematic illustration of the origin of Stokes-like shift and carrier localization in InGaN.

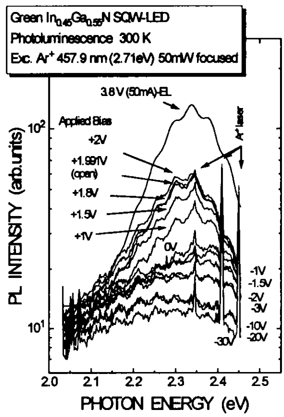

Fig. 6 PL spectra of an $In_{0.45}Ga_{0.55}N$ SQW LED as a function of external bias. Carriers are excited only in the QW.

corresponds to that taken under open-circuit condition. By applying -2 V reverse bias, the PL intensity decreases to one-third of that for the +2 V bias. The emission vanishes for a reverse bias of -10 V. However, it is difficult to judge the direction of the peak energy shift, since the QW thickness is only 3 nm.

EL spectra of the SQW LED's are shown in Fig. 7(a) and 7(b) as a function of driving current. The

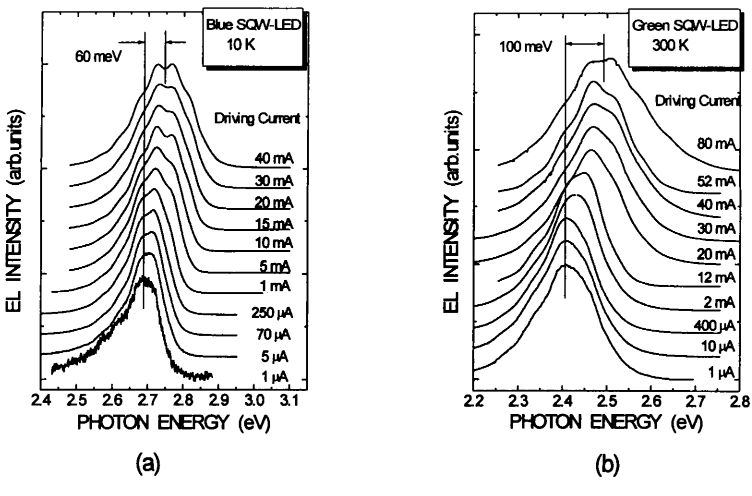

Fig. 7 EL spectra of (a) blue and (b) green InGaN SQW LED's as a function of driving current.

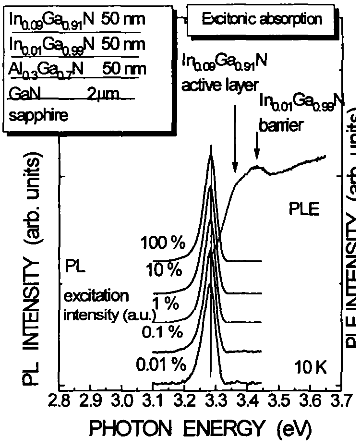

Fig. 8 PL and PLE spectra of 3D $In_{0.09}Ga_{0.91}N$ layer at 10 K.

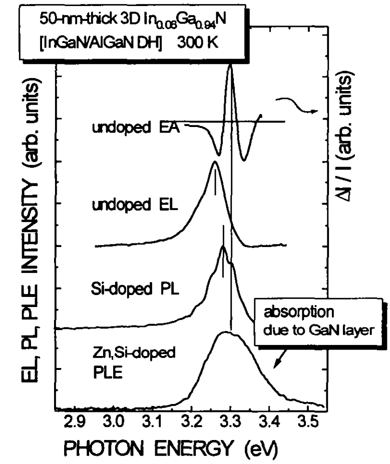

Fig. 9 Optical spectra of 3D $In_{0.06}Ga_{0.94}N$ device structures at RT.

emission intensity increases approximately linearly by increasing driving current. A similar relation between the intensity and excitation level was observed for the PL/EL spectra of all the QW and 3D structures investigated herein. The emission intensity is nearly constant from 10 K to RT in these SQW LED's. Note that the shoulder-like distinct fringes in the EL spectra are due to internal multiple reflections at the surface and n-GaN/sapphire interface. The EL peaks shifted to higher energy by 60 meV and 110 meV. These blueshifts could be explained by piezoelectric field induced QCSE assuming the appropriate degree of residual strain. However, both EL spectra showed spectral broadening with the blueshift (increasing the current). This phenomena cannot be explained only by the QCSE in terms of the Coulomb screening of the piezoelectric field by current injection. Therefore the blueshift in the EL peak energy may be due to combined effects of the QCSE (screening of the piezoelectric field and built-in field) and band-filling of the local potential minima produced by the potential fluctuations.

Supporting evidence for the potential fluctuation in InGaN materials was also obtained from the optical properties of 3D bulk InGaN layers with small x, where the QCSE is negligible, as follows. Fig. 8 shows PL and PLE spectra at 10 K of a 50 nm-thick 3D $In_{0.09}Ga_{0.91}N$ epilayer grown on $In_{0.01}Ga_{0.99}N$ / $Al_{0.3}Ga_{0.7}N$ stacked buffer layer [13]. The PL peak energy is unchanged by changing the excitation intensity up to 4 orders of magnitude. The PL peak at 3.28 eV is effectively excited by the FE absorption in both the active and barrier layers shown by the arrows followed by a band-to-band (B-B) continuum. The PL peak is located at the lower energy tail of the FE absorption. The FWHM of the FE resonance in the $In_{0.09}Ga_{0.91}N$ active layer is estimated to be about 75 meV, showing a large potential fluctuation. The Stokes-like shift is 85 meV [13].

Various optical spectra of the 50 nm-thick 3D $In_{0.06}Ga_{0.94}N$ layers at RT are summarized in Fig. 9. The EA spectrum of the undoped layer exhibits a derivative-like, broadened resonance structure. The broadening is attributed to the potential fluctuations in InGaN. This is proved later by the spatially-resolved CL measurements. The FE energy in 3D $In_{0.06}Ga_{0.94}N$ at RT is 3.298 eV, which agrees well with the PLE peak energy in $In_{0.06}Ga_{0.94}N$ codoped with Si and Zn, as shown in the bottom trace. The decrease of the PLE signal in the higher-energy side is due to the absorption by the top *p*-GaN layer. Nevertheless, the PLE spectrum exhibits an excitonic absorption even at RT, as is the case at 10 K (Fig. 8). Again in the undoped 3D $In_{0.06}Ga_{0.94}N$ device structure, the spontaneous EL peak appeared in the lower energy tail of the FE resonance even at RT, showing a Stokes-like shift of 40 meV [13]. Note here that radiative decay of localized excitons in 3D InGaN layers has been reported by TR-PL measurements [33], temperature-dependent PL measurements [34], and modulation spectroscopy measurements [13].

Potential inhomogeneity and exciton localization in InGaN

There are several mechanisms for carrier localization in QW's as shown in Fig. 5; (i) monolayer thickness fluctuation, (ii) spatial compositional (or strain) undulation, and (iii) complete phase separation. These are referred to as cases A, B, and C, respectively hereafter. The case A and relatively weak potential fluctuation (case B) usually produce a weak potential undulation in QW's. A strong complete phase separation (case C) produces well-defined quantum dots (Q-dots), Q-disks, or segmented QW's (SgQW's) depending on the lateral size. The case in between B and C produces a strong potential undulation where a Q-disk potential or segmented QW condition is sustained.

In order to figure out the spatial distribution of the emission, three 3 nm-thick $In_xGa_{1-x}N$ SQW's (x=0.05, 0.2, and 0.5) capped by a 6-nm-thick GaN layer were prepared. The growth parameters were exactly the same as those for the blue and green SQW LED's [1] except for the GaN capping.

First we observed cross-sectional TEM, and found very abrupt heterointerfaces between the SQW and GaN in all samples [15]. The TD density was less than 10^9 cm^{-2}. Abrupt heterointerfaces were also observed in $In_{0.2}Ga_{0.8}N$ / $In_{0.05}Ga_{0.95}N$ MQW LD wafer [1,13]. The atomic force microscopy (AFM) images of GaN-capped and uncapped $In_{0.5}Ga_{0.5}N$ SQW's were also examined. The GaN-capped SQW exhibited a flat surface with nanoscale holes owing to TD's. Also, several monolayers step structure presumably due to spiral growth initiated by TD's [35] were found [15]. On the other hand, the uncapped bare SQW exhibited many grooves (10-50 nm diam., 1-2 nm depth). These grooves are considered to be areas of reevaporated InN-rich materials in the SQW since the MOVPE recipe was terminated just after the SQW growth at the growth temperature where the vapor pressure of InN is higher than that of GaN.

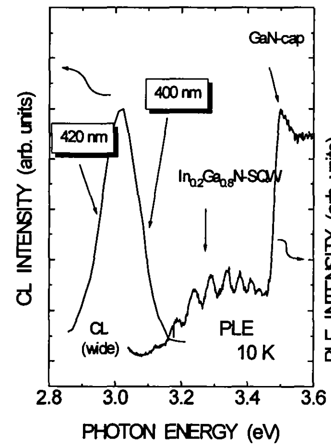

Fig. 10 Wide-area CL spectrum and its PLE spectrum of $In_{0.2}Ga_{0.8}N$ SQW at 10 K.

A wide-area (500x500 μm^2) PL spectrum and its PLE spectrum of the GaN-capped $In_{0.2}Ga_{0.8}N$ SQW taken at 10 K are shown in Fig. 10. The PL peak energy was 3.017 eV, and the FWHM is nearly 130 meV. The averaged FE resonance energy in the SQW is 3.28 eV, showing a Stokes-like shift of 270 meV at 10 K. These values are larger than those reported before [14,15].

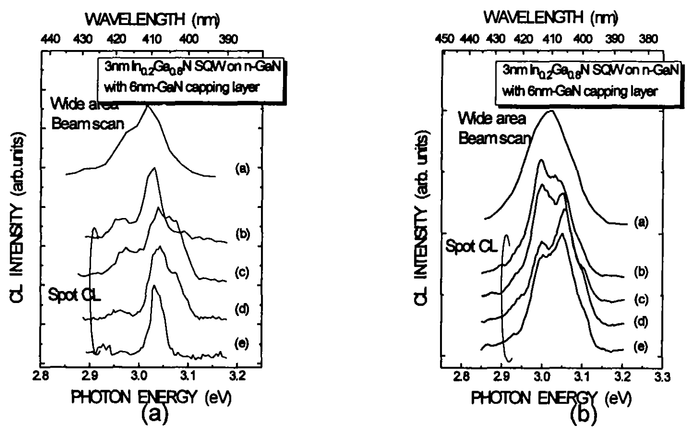

Fig. 11 Wide-area CL spectra and spot CL spectra of $In_{0.2}Ga_{0.8}N$ SQW at 10 K.

A wide-area (10x10μm^2) integrated scanning CL spectrum from two different positions of the same sample measured at 10 K is shown in Fig. 11 (a) and (b). As is the case with the result reported before [15], CL peak energies obtained from limited spot areas (~500 x 60 nm^2) varied from position to position. The FWHM values of the spot CL peaks (~30 meV) are much smaller than that of the wide-area scanning CL peak (~90 meV [15] or 130 meV). Note that the spectral resolution is as large as 15 meV. These results clearly show that the wide-area broadened CL (and PL) peak consists of sharper emission peaks having various peak energies, which are separated by 50 meV. The appearance of several CL peaks in the spectra (b)-(e) in Fig. 11(a) and(b) is not due to a multiple interference effect. Therefore, there exist several nanoscale *structures* having different net bandgap energies. This *structure* can act as segmented QW's, Q-disks, or Q-dots having compositional and/or size inhomogeneity depending on their lateral size.

Monochromatic scanning CL images of the GaN-capped $In_{0.2}Ga_{0.8}N$ SQW taken at wavelengths of 400 nm (3.100 eV) and 420 nm (2.952 eV), which correspond to the higher and lower energy side of the wide-area integrated CL peak at 411 nm (3.017 eV), indicated the following results [15]; (i) each bright area emitting CL consists of emissions from regions of less than 60 nm up to 400 nm in lateral size, (ii) some dark areas in one wavelength correspond to bright ones in the other wavelength, (iii) some areas exhibit both 400 and 420 nm CL emissions, and (iv) approximately 40% of the entire areas are dark at both wavelengths. These results can be explained by the existence of the potential undulation whose lateral size/interval is smaller than 60 nm. This value is the spatial resolution of the system, and is essentially limited by the carrier diffusion length.

The *structures* having lateral sizes smaller than the exciton resonance wavelength, which is the emission wavelength divided by the refractive index and corresponds approximately to 160 nm in this case, are defined as Q-disks [18]. In Q-disks, the spontaneous emission lifetime of excitons is longer than that in two-dimensional QW's [18]. Here we should mention than both Q-disks and SgQW's lase via EHP with the Coulomb enhancement [19,36], since there is no or very weak carrier/exciton confinement in lateral directions. Therefore we call hereafter the *structure* as Q-disks and/or SgQW's, because we cannot define their absolute sizes. Note that the electron and hole wave functions in Q-disks or SgQW's are quantized at least with respect to the z-direction. The result (iv) can also be interpreted as existence of Q-disks superimposed in the large scale inhomogeneity expanding up to 400 nm in lateral size.

At 420 nm, the bright area density is about 5x10^8 cm^{-2}, which is close to the TD density. Also, the spacing between the large bright areas is also close to the TD spacing. Very recently, Sato et al. [37] showed featureless CL images for $In_{0.14}Ga_{0.86}N$ layers grown on homoepitaxially-grown thick GaN layers having very low TD densities. Their result was quite different from the inhomogeneous CL images [15]. Thus the TD's are likely to act as some driving forces of the potential fluctuation in InGaN. The monochromatic CL image of $In_{0.05}Ga_{0.95}N$ SQW also exhibited an inhomogeneous fine structure, and the Stokes-like shift was nearly 60 meV. The *structure* size was smaller than that of the SQW with x=0.2.

There are two possible origins of the potential fluctuation; (1) compositional inhomogeneity and (2) monolayer thickness fluctuation. If we assume a coherent growth of InGaN [10], relative change in the x value is estimated to be less than a few % to reproduce a bandgap change of nearly 100 meV. Next if we assume the monolayer thickness fluctuation without any compositional inhomogeneity, the energy difference between two regions having different well thicknesses might be a sum of the change in quantized energy level and change in the Stark shift due to piezoelectric QCSE. Since several groups [15,35] have shown 4-6 monolayer thickness steps in AFM images of GaN-capped SQW, it might explain the appearance of several sharp CL peaks shown in Fig. 11. If we

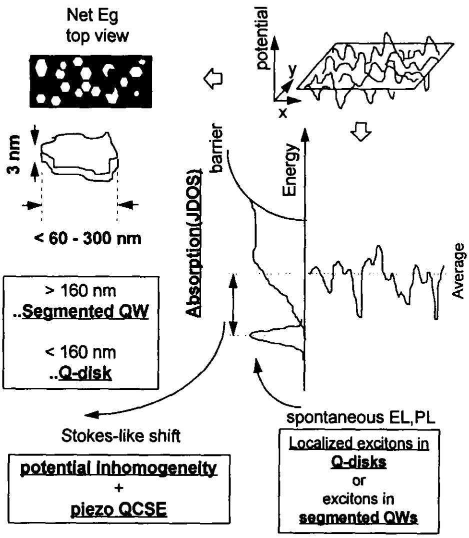

Fig. 12 Schematic drawing of the potential inhomogeneity in InGaN QW's

again assume coherent growth, InN-rich regions may suffer larger piezoelectric QCSE. In both cases, the carrier localization due to the potential fluctuation is enhanced by the Stark effect. In this case, the electronic confinement system can be referred to as Stark-enhanced Q-disk/SgQW potential.

It has been argued that InGaN QW's contained InN-rich Q-dots having a lateral size of a few nm [14,17,38,39]. Since the spatial resolution of our CL system is 60 nm, it is impossible to discuss that question. The large Stokes-like shift (260 meV), which may contain both potential inhomogeneity and piezoelectric QCSE, indicates that other parts of the SQW could have larger bandgap energies. Those parts would be seen as dark areas at the wavelengths monitored herein provided that the diffusion length is short enough. It follows from the result (iv) that the real area emitting CL is much smaller than the bright area observed. Anyway, it is proved that electrons injected in such widegap areas move to narrow gap areas to emit CL. Such Q-disks or SgQW's can enhance the emission efficiency in the QW due to a limitation of exciton movement in small spaces, which can reduce nonradiative pathways. Schematic representation of the potential fluctuation, Stokes-like shift, and localized tail states in InGaN QW's is shown in Fig. 12.

Localized excitons in mesoscopic semiconductor quantum disks in inhomogeneous $In_xGa_{1-x}N$ QW's

The spontaneous emission peak from InGaN QW's and 3D layers is assigned as being due to the recombination of excitons localized at potential minima as follows. We compared the environmental conditions for excitons assuming that LED devices are operated under the catalogue DC values (I=20 mA) or less. (1) As is the case with GaN, few LO phonons are thermally active in InGaN at RT due to their large energies (91.8 meV for GaN [23] and 73.6 meV for InN [40]). (2) Because the InN molar fraction x of the undoped DH LED is as small as 0.06, which can be deduced to be nearly 3% provided that the 3D layer is strained, E_{ex} of a 3D layer is considered to be nearly the same as that of GaN (26 meV) [25-28].

For 3D DH LED's, (3) the injected carrier density for the dc EL operation is estimated to be less than 10^{17} cm^{-3} using the values of active layer thickness (50 nm), injected current density, and the emission decay time (τ=1 ns). (4) The piezoelectric field is weaker than the critical value (7.6×10^4 V/cm), since there is less than 0.3 % of lattice mismatch. Under these conditions, 3D FE's can survive at RT. The localization energy for the particular LED was 40 meV at RT, which is larger than the thermal energy at RT. Note that emission is either localized or nearly free depending on the sample quality.

Two restrictions (3) and (4) are critical for QW's, since there exist strong piezoelectric and built-in field, and high carrier density is established in very thin 3 nm-thick SQW's. It is known that excitons can survive up to RT in QW's because of the increase of E_{ex} due to the confinement of the wave functions. Thus we have calculated E_{ex} in 3 nm-thick GaN QW's by a variational approach taking the elecron-hole pair motion in the QW into account [41]. The value obtained (47 meV) is about 1.8 times larger than that in the 3D case, implying that the electric field to dissociate FE's in the QW's is as high as 6.0×10^5 V/cm. If we assume the entire Stokes-like shift is due to piezoelectric QCSE, the piezoelectric field exceeds this value. However, both the QW's and 3D layers still have areas having a potential minimum even at RT, where carriers or excitons are spatially localized. The spectral broadening due to the increase of the driving current shown in Fig. 7 is a sign of the band-filling of such regions, where the electric field is weakened by the forward current injection. Also, the carrier density in the SQW is estimated to be about 1.2×10^{18} cm^{-3} (I=20 mA, τ=3 ns). This value is comparable to the critical charge density for FE's in 3D GaN. Thus the observation of the excitonic emission seems to be possible in the potential minima, where the electron-hole distance is shorter than that in the 3D case. The improvement of the emission intensity in QW's compared to the 3D case [13] may be attributable to the increased E_{ex} and oscillator strength of localized excitons or carriers in the QW's.

Optical gain in cw LD's with relatively homogeneous and inhomogeneous MQW's

Optical gain spectra of CW1 and CW2 are compared in Fig. 13(a) and 13(b), respectively. The arrows on the EA spectra indicate the averaged FE resonance energy in the QW's. The stimulated emission peak energy of CW1 is close to the FE resonance energy. Although the Stokes-like shift for the spontaneous EL of CW1 is larger than that of CW2, the gain spectrum of CW1 can be well explained by the EHP picture [19,22,42,43], and the FWHM of the gain peak for CW1 is smaller than that of CW2. This means that potential fluctuation for CW1 is smaller than that of CW2, and most of the Stokes-like shift of CW1 may come from the piezoelectric QCSE. It is obvious that CW2 contains more In in the well. The appearance of sharp stimulated emission and gain peaks on the spontaneous EL peak for CW2, which appeared for high pumping energy density or long excitation-stripe lengths, indicates that the Stokes-like shift cannot be explained only by the piezoelectric QCSE, and that there exist actual energy states below the averaged FE

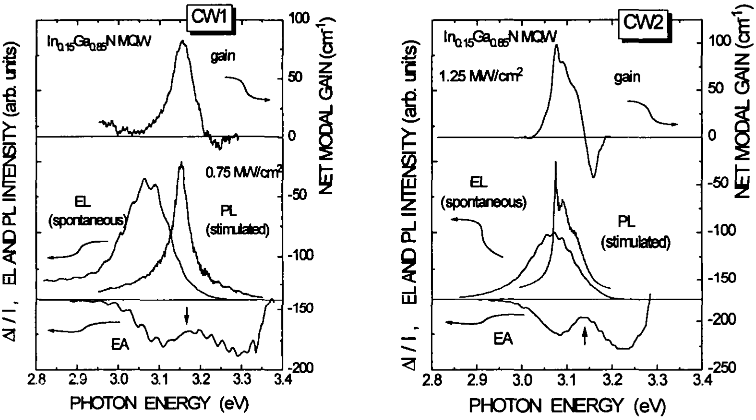

(a) CW1 (b) CW2

Fig. 13 Optical gain spectra of $In_{0.15}Ga_{0.85}N$ CW MQW LD's with different degree of inhomogeneity.

resonance energy. A remarkable absorption peak above the FE resonance energy appeared simultaneously with the appearance of the sharp gain peaks. This might be due to the effective resonance between two degenerate levels and one undegenerate level (three-level lasing model) [36,44,45]. This means that CW2 is considered to lase by EHP in segmented QW's or Q-disks. The J_{th} value for CW1 is smaller than that of CW2, and therefore it is desireble to use entire QW planes as gain media for higher performance LD operation.

CONCLUSION

Emission mechanisms of the device-quality InGaN SQW and MQW structures grown on sapphire substrates without any ELOG base layers were investigated. The $In_xGa_{1-x}N$ layers showed various degrees of spatial potential fluctuation. The degree of fluctuation changed around nominally x=0.2 (nearly 8-10 % for the strained $In_xGa_{1-x}N$). The potential undulation induces the energy tail states both in QW and 3D InGaN, showing a large Stokes-like shift combined with the redshift due to piezoelectric QCSE. The spontaneous emission from undoped InGaN SQW LED's, undoped 3D DH LED's, and MQW LD wafers was assigned as being due to the recombination of excitons localized at the potential minima, whose area was determined by the monochromatic CL mapping to vary from less than 60 nm up to 300 nm in lateral size. The lasing mechanisms of the cw $In_{0.15}Ga_{0.85}N$ MQW LD's having small potential fluctuation can be described by the well-known EHP picture with strong Coulomb enhancement while LD's having strongly inhomogeneous MQW exhibited a sharp gain peak produced in a limited area, tail states, in the QW planes. The inhomogenous MQW LD's are considered to lase by EHP in segmented QW's or Q-disks. It is desirable to use entire QW planes as gain media for higher performance LD operation. Note that use of InGaN QW's with small potential fluctuation results in lasing operation while GaN QW's have not shown electrically-pumped lasing.

ACKNOWLEDGMENTS

The authors are grateful to Dr. T. Uenoyama, Dr. S. Keller, Dr. J. Speck, Dr. M. Sugawara, Dr. T. Azuhata and Professor K. Suzuki for stimulating discussions. The authors would like to thank Dr. S. Shirakata for instruction about PR measurements. They are also grateful to Professor H. Nakanishi, Professor H. Ikoma, Professor U. K. Mishra, Professor L. A. Coldren and Professor S. P. DenBaars for continuous encouragement.

REFERENCES

1. Important data and references are cited in the textbook [S. Nakamura and G. Fasol, The Blue Laser Diode, (Springer, Berlin, 1997)]; recent data are from S. Nakamura, M. Senoh, S. Nagahama, N. Iwasa, T. Yamada, T. Matsushita, Y. Sugimoto, H. Kiyoku, Jpn J. Appl. Phys. **36**, L1059 (1997); They further adopted a modulation-doped superlattice cladding layers and ELOG layers, and the accelaration test has been done at 50°C [S. Nakamura, presented at The 2nd Internati. Conf. on Nitride Semiconductors, Tokushima, Japan, Oct. 27-31, 1997].
2. I. Akasaki, S. Sota, H. Sakai, T.Tanaka, M. Koike and H. Amano, Electron. Lett. **32**, 1105 (1996).
3. K. Itaya, M. Onomura, J. Nishio, L. Sugiura, S. Saito, M. Suzuki, J. Rennie, S. Nunoue, M. Yamamoto, H. Fujimoto, Y.Kokubun, Y. Ohba, G.Hatakoshi, and M. Ishikawa, Jpn. J. Appl. Lett. **35**, L1315 (1996).
4. G. E. Bulman, K. Doverspike, S. T. Sheppard, T. W. Weeks, H. S. Kong, H. M. Dieringer, J. A. Edmond, J. D. Brown, J.T. Swindell, and J. F. Schetzina, Electron. Lett. **33**, 1556 (1997).
5. A. Kuramata, K. Domen, R. Soejima, K. Horino, S. Kubota, and T. Tanahashi, Proc. 2nd Internati. Conf. on Nitride Semiconductors, (Tokushima, Japan, 1997) pp.450.
6. M. P. Mack, A. Abare, M. Aizcorbe, P. Kozodoy, S. Keller, U. K. Mishra, L. A. Coldren, and S. P. DenBaars, Mater. Res. Soc. Internet J. Nitride Semicond. Res. **2**, 41 (1997).
7. A. Koukitsu, N. Takahashi, T. Taki, and H. Seki, Jpn. J. Appl. Phys. **35**, L673 (1996).
8. I-hsiu Ho and G. B. Stringfellow, Appl. Phys. Lett. **69**, 2701 (1996).
9. T. Matsuoka, Appl. Phys. Lett. **71**, 105 (1997).
10. T. Takeuchi, H. Takeuchi, S. Sota, H. Sakai, H. Amano, and I. Akasaki, Jpn. J. Appl. Phys. **36**, L177 (1997); Proc. 2nd Internati. Conf. on Nitride Semiconductors, (Tokushima, Japan, 1997) pp.450 .
11. S. Chichibu, T. Azuhata, T. Sota and S. Nakamura, J. Appl. Phys. **79**, 2784 (1996); Proc. Int. Symp. On Blue Laser and Light Emitting Diodes (Ohmsha, Tokyo, 1996), pp.202; S. Chichibu, H. Okumura, S. Nakamura, G. Feuillet, T. Azuhata, T. Sota and S. Yoshida, Jpn. J. Appl. Phys. **36**, 1976 (1997).
12. B. Monemar, J. P. Bergman, H. Amano, I. Akasaki, T. Detchprohm, K. Hiramatsu, and N. Sawaki, Proc. Int. Symp. on Blue Laser and Light Emitting Diodes (Ohmsha, Tokyo, 1996), pp. 135.
13. S. Chichibu, T. Azuhata, T. Sota, and S. Nakamura, 38th Electron. Mater. Conf., Santa Barbara, CA, June 26-28, 1996, Late News Paper W-10; Appl. Phys. Lett. **69**, 4188 (1996); Mater. Res. Soc. Symp. Proc. Vol. **449**, 653 (1997); Appl. Phys. Lett. **70**, 2822 (1997).
14. Y. Narukawa, Y. Kawakami, Sz. Fujita, Sg. Fujita, and S. Nakamura, Phys. Rev. B **55**, R1938 (1997); Y. Narukawa, Y. Kawakami, M. Funato, Sz. Fujita, Sg. Fujita, and S. Nakamura, Appl. Phys. Lett. **70**, 981 (1997).
15. S. Chichibu, K. Wada, and S. Nakamura, Appl. Phys. Lett. **71**, 2346 (1997).
16. M. Smith, G. Chen, J. Y. Lin, H. Jiang, M. A. Khan, and Q. Chen, Appl. Phys. Lett. **69**, 2837 (1996).
17. F. Scholz, V. Haerle, F. Steuber, A. Sohmer, H. Bolay, V. Syganow, A. Doernen, J. -S. Im, A. Hangleiter, J. Y. Duboz, P. Galtier, E. Rosencher, O. Ambacher, D. Brunner, and H. Lakner, Mater. Res. Soc. Symp. Proc. Vol., **449**, 3 (1997).
18. M. Sugawara, Phys. Rev. B **51**, 10743 (1995).
19. For a review, see for example, H. Haug and S. W. Koch, Quantum Theory of the Optical and Electronic Properties of Semiconductors, (World Scientific, Singapore, 1990) and W. W. Chow, S. W. Koch, and M. Sargent III, Semiconductor-Laser Physics, (Springer, Berlin, 1994); W. W. Chow, A. F. Wright, and J. S. Nelson, Appl. Phys. Lett. **68** , 296 (1996).
20. M. Cardona, in Modulation Spectroscopy, Solid State Physics Suppl.11, ed. S. Seitz, D. Turnbull and H. Ehrenreich (Academic, New York, 1969); D. E. Aspnes, Handbook on Semiconductors, ed. T. S. Moss (North-Holland, Amsterdam, 1980) Vol. 2, Chap. 4A, p. 109; D. E. Aspnes, Surf. Sci. **37**, 418 (1973).
21. K. L. Shaklee and R. F. Leheny, Appl. Phys. Lett. **18**, 475 (1971); K. L. Shaklee, R. F. Leheny, and R. E. Nahory, Appl. Phys. Lett. **19**, 302 (1971).
22. T. Deguchi, T. Azuhata, T. Sota, S. Chichibu, and S. Nakamura, European Mater. Res. Soc. 1997 Spring Meeting, Strasbourg, France, Jun.16-20, 1997, L-XIII-3; to be published in Mater. Sci. Engineering B.
23. T. Azuhata, T. Sota, K. Suzuki, and S. Nakamura, J. Phys. Condens. Mat. **7**, L129 (1995); T. Azuhata, T. Matsunaga, K. Shimada, K. Yoshida, T. Sota, K. Suzuki, and S. Nakamura, Physica B **219/220**, 493 (1996).

24. S. Chichibu, T. Mizutani, T. Shioda, H. Nakanishi, T. Deguchi, T. Azuhata, T. Sota, and S. Nakamura, Appl. Phys. Lett. **70**, 3440 (1997).
25. S. Chichibu, A. Shikanai, T. Azuhata, T. Sota, A. Kuramata, K. Horino, and S. Nakamura, Appl. Phys. Lett. **68**, 3766 (1996); A. Shikanai, T. Azuhata, T. Sota, S. Chichibu, A. Kuramata, K. Horino, and S. Nakamura, J. Appl. Phys. **81**, 417 (1997).
26. M. Suzuki, T. Uenoyama, and A. Yanase, Phys. Rev. B **52**, 8132 (1995).
27. R. Dingle, D. D. Sell, S. E. Stokowski, and M. Ilegems, Phys. Rev. B **4**, 1211 (1971).
28. B. Monemar, Phys. Rev. B **10**, 676 (1974).
29. S. Shirakata and S. Chichibu, J. Appl. Phys. **80**, 2043 (1996).
30. J. S. Im, V. Haerle, F. Scholz, and A. Hangleiter, MRS Internet J. Nitride Semicond. Res. **1**, 37 (1996).
31. D. L. Smith and C. Mailhiot, Phys. Rev. Lett. **58**,1264(1987).
32. The piezoelectric field was calculated with the values of piezoelectric constants of GaN according to M. P. Halsall, J. E. Nicholls, J. J. Davies, B. Cockayne, and P. J. Wright [J. Appl. Phys. **71**, 907 (1992)], and the Stark shift due to the electric field was calculated by the variational method neglecting exciton binding energy. Calculations are based on work by D. A. Miller, D. S. Chemla, T. C. Damen, A. C. Gross, W. Wiegmann, T. H. Wood, and C. A. Burrus [Phys. Rev. Lett. **53**,2173(1981) and Phys. Rev. B **32**, 1043 (1985)].
33. C. I. Harris, B. Monemar, H. Amano, and I. Akasaki, Appl. Phys. Lett. **67**, 840 (1995).
34. T. Taguchi, T. Maeda, Y. Yamada, S. Nakamura, and G. Shinomiya, Proc. Int. Symp. On Blue Laser and Light Emitting Diodes (Ohmsha, Tokyo, 1996), p.372.
35. S. Keller, B. P. Keller, M. S. Minsky, J. E. Bowers, U. K. Mishra, S. P. DenBaars, and W. Seifert, presented at The 2nd International Conf. on Nitride Semiconductors, Tokushima, Japan, Oct.27-31, 1997, Session M2-5; and also a private communication.
36. T. Uenoyama, Phys. Rev. B **51**, 10228 (1995); and also a private communication.
37. H. Sato, T. Sugahara, Y. Naoi, and S. Sakai, Proc. 2nd Internati. Conf. on Nitride Semiconductors, (Tokushima, Japan, 1997) p. 28.
38. C. Kisielowski and Z. Liliental-Weber (private communication); they have observed a dot-like nanoscale compositional disorder in the SQW LED wafers using the electron scattering potential mapping method.
39. F. A. Ponce, presented at European Mater. Res. Soc. 1997 Spring Meeting, Strasbourg, France, Jun.16-20, 1997, No. L-VII.4 (late news).
40. H. -J. Kwon, Y. H. Lee, O. Miki, H. Yamano, and A. Yoshida, Appl. Phys. Lett. **69**, 937 (1996).
41. T. Sota, S. Chichibu, and S. Nakamura (private communication). The E_{ex} value in $GaN/Al_{0.1}Ga_{0.9}N$ QW was calculated by the variational method according to G. Bastard, E. E. Mendez, L. L. Chang, and L. Esaki [Phys. Rev. B **26**, 1974 (1982)]. In the calculation, we started from the Hamiltonian suitable to QW's including mass and dielectric constant anisotropy, assuming an infinite barrier height to simplify the calculation. After variable transformations for Z coordinates (perpendicular to the QW plane) which formally remove the mass anisotropy in the Hamiltonian, E_{ex} was calculated using the trial function for the excitonic relative motion given by $\exp\{-[\rho^2+(Z_e-Z_h)^2]^{1/2}/\lambda\}$, considering the fact that the 3D exciton Bohr radius is as small as 3.4 nm. Here λ is the variational parameter, ρ is the absolute value of the relative position of electron and hole in the QW plane, and $Z_e(Z_h)$ is the transformed Z coordinate of the electron (hole).
42. G. Frankowsky, F. Steuber, V. Haerle, F. Scholz, and A. Hangleiter, Appl. Phys. Lett. **68**, 3746 (1996).
43. M. Kuball, E. -S. Jeon, Y. -K. Song, A. Nurmikko, P. Kozodoy, A. Abare, S. Keller, L. A. Coldren, U. K. Mishra, S. P. DenBaars, and D. A. Steigerwald, Appl. Phys. Lett. **70**, 2580 (1997).
44. W. Chen, M. Fritze, A. V. Nurmikko, D. Ackley, C. Covard, and H. Lee, Phys. Rev. Lett. **64**, 2434 (1990).
45. J. F. Mueller, Phys. Rev. B **42**, 11189 (1990).